Heliyon 7 (2021) e06882

Contents lists available at ScienceDirect

Heliyon

journal homepage: www.cell.com/heliyon

Research article

Mineralogical-geochemical study of the anionic competition effect on the octacalcium phosphate reaction into fluorapatite

Alfredo Idini, Franco Frau *

Department of Chemical and Geological Sciences, University of Cagliari, 09042, Monserrato, CA, Italy

ARTICLE INFO

Keywords:
Octacalcium phosphate
Anionic competition
Fluorapatite formation
Fluoride uptake from aqueous solution

ABSTRACT

The unstable compound octacalcium phosphate (OCP) is one of the crystalline precursors of the apatite mineral series composed by hydroxyapatite, fluorapatite and chlorapatite. The feature of OCP to react into apatite, depending on the media conditions, has been mainly exploited for biomedical applications as bone and tooth substitute material. Recently, some important applications of OCP have been documented: e.g. as electrode material for supercapacitors and as fluoride remover reagent for environmental purposes. With the aim of deepening the property of OCP to be the crystalline precursor of apatite and assessing if and how the anionic competition can influence the formation of the different apatite end-members, the OCP → apatite reaction has been here investigated placing 0.223 mmol of OCP in 50 mL aqueous solution with 0.368 mmol of dissolved fluoride, chloride, hydroxyl and carbonate anions (fluoride alone, fluoride with each of the other anions, and all the anions together) at room temperature. The post-experiment analyses of solid and liquid phases, conducted by using XRD, ESEM and ICP-OES, show that fluoride is always the main anion removed from solution during the OCP transformation reaction. The precise mineralogical characterization of solid phases formed, performed using the Rietveld algorithm, shows that fluorapatite is always the main resulting apatitic phase, followed by hydroxyapatite. Taking into account the different application fields of OCP, these results could be significant in better defining the OCP → apatite reaction in aqueous solutions where different competing anions are involved.

1. Introduction

The apatite supergroup is composed of 43 minerals (formally divided into five groups: apatite, hedyphane, belovite, britholite and ellestadite) which have general chemical formula $M1_2M2_3(TO_4)_3X$ (Z = 2). The M sites (M1 in coordination IX, M2 in coordination VII) host mainly calcium (Ca^{2+}) and lead (Pb^{2+}) and a large number of other cations, the T site (coordination IV) can host mainly phosphorous (P^{5+}), arsenic (As^{5+}), vanadium (V^{5+}), and the X site is occupied by fluoride (F^-), chloride (Cl^-) and hydroxyl (OH^-) anions (Supplemental Data Fig. SD1) (Pasero et al., 2010).

In the apatite group, hydroxyapatite (HAp, $Ca_5(PO_4)_3OH$), fluorapatite (FAp, $Ca_5(PO_4)_3F$) and chlorapatite (ClAp, $Ca_5(PO_4)_3Cl$) are the ideal end-members of a complete solid solution. The natural apatite is mostly fluorapatite where F^- can be partially replaced by OH^- and Cl^- in the X site (Hughes and Rakovan, 2015). Moreover, several studies report that many different substitutions in the M and T sites can occur both in natural and synthetic samples, one of which is the entrance of the carbonate anion (CO_3^{2-}) in partial substitution of phosphate, which is geologically well documented in the sedimentary phosphorite deposits, composed primarily of francolite, the carbonate-rich variety of FAp (Jarvis et al., 1994). In addition to the great importance of apatite in the geological ambit (Rakovan and Pasteris, 2015), the related compound called calcium orthophosphate (Dorozhkin, 2016) is extensively studied in medicine and biology because the inorganic part of mammal hard tissues is composed of bioapatite, a calcium-phosphate mineral with apatitic structure (Sakae et al., 2015). Common chemical features of bioapatite include: (i) the presence of some hydrogen phosphate (HPO_4^{2-}) and/or partial substitution (around 7–9 %) of carbonate instead of phosphate, both substitutions causing a calcium deficiency in the structure (i.e. a calcium-deficient apatite); (ii) the OH^- depletion in the anionic X site (Wopenka and Pasteris, 2005). However, the bioapatite can show very different Ca/P and OH/F ratios, depending on the type of biological hard tissue. Among the calcium orthophosphate compounds, the octacalcium phosphate (OCP, $Ca_8(HPO_4)_2(PO_4)_4 \cdot 5H_2O$, 892.468 g/mol) has been extensively studied, exploiting its biomedical properties as bone and tooth substitute material in various forms since OCP is one of the mineralogical precursors of apatite (Arellano-Jiménez et al., 2009)

* Corresponding author.
E-mail address: frauf@unica.it (F. Frau).

https://doi.org/10.1016/j.heliyon.2021.e06882
Received 3 May 2020; Received in revised form 29 July 2020; Accepted 19 April 2021

and bioapatite (Suzuki, 2013). In fact, in alkaline aqueous solution, OCP tends to transform into HAp or, depending on medium conditions, into bioapatite. The mechanism of mineralogical transformation has been debated in several studies, but the articles of Xin et al. (2006) and Carino et al. (2018) clarified that the solid-state transformation and then the epitaxial growth of HAp onto OCP are the main mechanisms involved.

Recent studies have shown that OCP reacts in the presence of fluoride in solution to form FAp (Idini et al., 2019), and this reaction occurs also in biological conditions. The formation of FAp, instead of bioapatite, in mammal hard tissues causes different pathologies called skeletal and dental fluorosis (Everett, 2011). Skeletal and non-skeletal fluorosis pathologies (Ozsvath, 2009) are a well-known issue in many countries around the globe that affect more than two hundred million people (Ayoob and Gupta, 2006). The World Health Organization (WHO) indicates the fluoride-rich groundwaters as the main source of the excessive intake of fluorine by people, and the WHO guidelines for drinking-water quality (GDWQ) adopt a fluoride concentration of 1.5 mg/L as the permissible limit for human consumption (Fawell et al., 2006). As reported in the literature (Idini et al., 2019, 2020), in the frame of the FLOWERED project (www.floweredproject.org, Horizon2020 program funded by the European Commission) the use of OCP has been applied to uptake high dissolved fluoride from groundwater through the mineralogical transformation into FAp.

To the best of our knowledge and despite the vast literature about the application of the OCP → apatite reaction (e.g. to obtain biomaterials, electrodes for supercapacitors, to defluoridate fluoride-rich groundwater for drinking purposes), there is a lack of scientific knowledge about the behaviour of OCP as the crystalline precursor of apatite in the presence of different anions necessary to form each end-member of the apatite mineral series. Because of that, the two focuses of the study presented here are: (i) to understand how OCP reacts in the presence of equivalent molar concentrations of F^-, Cl^-, OH^- and carbonate species (HCO_3^- + CO_3^{2-}); (ii) to assess the effect of the anionic competition and determine which one of the apatite end-members is favoured in the OCP transformation reaction, and consequently indicate the possible implications of the OCP use in aqueous solutions (e.g. treatment of chemically complex fluoride-rich waters).

2. Materials and methods

All the chemicals used for the OCP synthesis and the anionic competition experiments were of analytical grade (Carlo Erba Reagents S.r.l., RPE grade, ACS quality); ultrapure water (Millipore, Milli-Q©, 18.2 MΩ cm) was used to prepare the solutions.

2.1. Synthesis of OCP

The OCP was synthesized following the method described by Idini et al. (2019), which briefly consists of the synthesis of dicalcium phosphate dihydrate (DCPD, $CaHPO_4 \cdot 2H_2O$) at room temperature using H_3PO_4 and $CaCO_3$, and the subsequent hydrolysis of DCPD into OCP in a solution of ultrapure water with a starting pH of 7.2. After aging at 60 °C for 65 h, the OCP was recovered from the solution as a white powder with particle size of 14–125 μm.

2.2. Anionic competition experiments

The anionic competition experiments were performed at room conditions in batch-mode using 50 mL conical flasks agitated through a rotor system at 40 rpm; 200 mg (0.223 mmol) of OCP were added to 50 mL solutions (solid/solution ratio = 4 g/L) with same molar concentrations of F^-, Cl^-, OH^- and carbonate species (HCO_3^- + CO_3^{2-}). The choice of the anionic concentrations in solution was based on the reaction of OCP into FAp:

$$Ca_8(HPO_4)_2(PO_4)_4 \cdot 5H_2O_{(OCP)} + 1.6F^- \rightarrow 1.6Ca_5(PO_4)_3F_{(FAp)} + 1.2HPO_4^{2-} + 5H_2O + 0.8H^+ \quad \text{(React 1)}$$

Considering React. (1) and the experimental setting, the F^- stoichiometric amount needed is 0.357 mmol for 0.223 mmol of OCP in 50 mL of solution, that is 7.14 mmol/L, but, in order to favour the kinetics of React. (1), a slightly higher F^- amount was used (0.368 mmol in 50 mL, that is 7.37 mmol/L corresponding to 140 mg/L), and the molarity of the other competing anions in solution was set up to that value. The time required because the OCP → FAp reaction goes close to completion in such conditions is less than 16 h, therefore every experiment was repeated, and pH and F^- concentrations monitored, after 16, 20 and 24 h (Idini et al., 2019) in order to verify the homogeneity of the measurements, for a total amount of 30 samples (Supplemental Data Table SD1). The complete chemical composition of solutions and solids was determined on the samples of the first trial after 24 h.

The salts used to provide the anions into solution were NaF, KOH, $NaHCO_3$ and NaCl. In order to have an exact amount of OH^-, the solution pH of each experiment was measured before the addition of OCP and after adding the other salts, and then KOH was added till the expected OH^- value was reached. The experiments were labelled as follows: No_Comp (absence of competitors; only F^- present in solution); Cl_Comp (F^- and Cl^- present together); OH_Comp (F^- and OH^- present together); Alk_Comp (F^- and carbonate species (HCO_3^- + CO_3^{2-}) present together); Tot_Comp (F^- and all anionic competitors simultaneously present in solution).

At the end of the experiments, the solids and solutions were separated through filtration and recovered to carry out the mineralogical characterization and chemical analysis.

2.3. Mineralogical and chemical analyses

The concentration of F^- in both solids (after their dissolution) and solutions was determined by a potentiometer (sensION TM + MM340, *HACH* LANGE) with Ion Selective Fluoride Electrode (ISE F– 9655C, *HACH* LANGE) and adding the TISAB III (*HACH*) solution to avoid interference of metallic complexes during the analysis. A portion of OCP before and after the experiments was dissolved in 67 % v/v HNO_3 and then diluted with ultrapure water for elemental analyses. The concentration of Na, Ca and P in solids was determined by inductively coupled plasma optical emission spectroscopy (ICP-OES, ARL Fisons 3520), while Cl^- was analysed by Ion Chromatography (IC, Dionex ICS3000). The initial bicarbonate concentration was calculated from alkalinity determined with the Gran method; in order to obtain the final bicarbonate concentration the contribution of phosphate was subtracted from alkalinity. The mineralogical characterization of solid phases, before and after the experiments, was performed collecting X-ray diffraction (XRD) patterns in the 3.5–55 °2θ angular range on an automated PANalytical X'Pert Pro diffractometer, with Ni-filtered Cu-$K_{\alpha 1}$ radiation (λ = 1.54060 Å), operating at 40 kV and 40 mA, using the X'Celerator detector. The XRD data were interpreted for phase identification with the X'Pert HighScore Plus software. Microphotographs and semi-quantitative chemical analyses of solids were collected with an environmental scanning electron microscope (ESEM, FEI Quanta 200) equipped with an energy dispersive X-ray spectrometer (EDS) and elaborated with the Pathfinder software (Thermo Fisher Scientific).

3. Results

3.1. Characterization of OCP

The XRD analysis of the synthesized compound identified it as OCP (Figure 1) in agreement with the two patterns of OCP listed in the Inorganic Crystal Structure Database (ICSD reference codes 00-026-1056 and 00-044-0778). All the peaks can be attributed to the OCP pattern, especially the OCP characteristic reflections at 4.74, 9.44 and 9.76 °2θ.

The crystallographic parameters, calculated with the DICVOL software (Boultif and Louër, 2004), converge towards the Triclinic system (P-1): a = 20.37, b = 9.78, c = 4.76 (Å); α = 90.7°, β = 92.9°, γ = 113.2°; V = 868.4 · 10^6 pm^3. The calculation was performed using 24 reflections with 3 % minimum relative intensities without unindexed peaks in the output. The agreement of the refinement, according to Smith and Snyder (1979), shows a Figure of Merit of 23.6.

It is worth saying that other authors have published OCP crystallographic refinement and reflections indexing (Table 1, Figure 1 and Table SD2 in the Supplemental Data), and there is an overall agreement about the belonging of OCP to the Triclinic system.

The ESEM images of OCP crystal aggregates (Figure 2) reveal that the synthesized OCP has a prismatic bladed habitus with an elongated axis (the a axis, according to our refinement). The crystals occur in radial aggregates (Figure 2).

The OCP spectra collected from different crystals show homogeneous elemental composition (Supplemental Data Figure SD2), and the quantitative ICP-OES chemical analysis, performed after dissolution of 1 g of OCP, shows a Ca concentration of 8.16 mmol/L and P concentration of 6.22 mmol/L, equivalent to a Ca/P molar ratio of 1.31 that is very close to the stoichiometric value of 1.33 in OCP.

3.2. OCP reaction into apatite: effect of anionic competition on aqueous solutions

The results of the anionic competition experiments are reported in Table 2. For convenience, due to the change of dissolved carbonate species as a function of pH, the carbonate species (HCO_3^- + CO_3^{2-}) are indicated with the general term "Alk" for alkalinity, and the corresponding experiment is Alk_Comp.

The main variations of anionic concentration in solution concern the decrease of F^- and OH^-, while Cl^- and (HCO_3^- + CO_3^{2-}) show a slight decrease (Table 2). The pH tends to the neutrality in every competition experiment regardless of the anionic species in solution. Similar results are observed in the "Tot_Comp" experiment, where the coexistence of all anions in solution is tested.

In order to compare the reduction of dissolved F^- in the different experiments, the removal of F^- from solution can be expressed as an empirical removal capacity (q_e) calculated through the formula:

$$q_e = (C_i - C_f)\ V/w \quad (1)$$

where q_e is the molar mass of F^- removed by mol of OCP (mol/mol), C_i and C_f are respectively the initial and final F^- concentrations (mol/L), V is the volume of solution (L) and w is the molar mass of OCP (Table 3). The maximum value of q_e = 1.33 calculated using Eq. (1) is reached in the No_Comp experiment, that is 17 % lower than the stoichiometric theoretical value of 1.6 in the OCP → FAp React. (1). The No_Comp experiment is taken as a reference for the other experiments, and therefore a percentage value of F^- removed equal to 100 % is attributed to it (Table 3, Figure 3).

The competition effect of Cl^- (Cl_Comp experiment) and (HCO_3^- + CO_3^{2-}) (Alk_Comp experiment) on F^- removal is very limited (respectively, q_e = 1.24, 93 % F^- removed; q_e = 1.29, 97 % of F^- removed), while the OH^- competition (OH_Comp experiment) is more evident (q_e = 1.10, 83 % F^- removed). When all anions are simultaneously present in solution (Tot_Comp experiment), the competition effect on F^- removal is even more noticeable (q_e = 1.06, 80 % F^- removed) (Table 3, Figure 3).

In every anionic competition experiment, as predicted by the OCP → FAp React. (1), some phosphorous is released into solution, while dissolved calcium should be nil. However, we have measured dissolved concentrations of P^{5+} and Ca^{2+} that are slightly higher than the stoichiometric values according to React. (1) (Table 3).

3.3. OCP reaction into apatite: effect of anionic competition on solid phases

The XRD analysis of the solid phases collected after the anionic competition experiments shows very similar patterns (Figure 4 and Figure SD3 in the Supplemental Data) that can be completely assigned, by means of peaks and whole diffraction profile fitting, to the apatite group minerals. Moreover, the OCP immersed in a deionized water solution (initial pH = 7.00, final pH = 5.62, absence of any of the competing anions) tends to retrocede to DCPD without apatite neoformation (Supplemental Data Figure SD4). Another phase that should be considered, taking into account the overall elemental composition of the experiments, is fluorite (CaF_2). In fact, due to the complete overlap of the fluorite XRD peaks with those of apatite in the investigated °2θ range, the minor precipitation of fluorite during the competition experiments cannot be ruled out only considering the XRD data. The presence, or not, of fluorite will be later discussed according to the ESEM and chemical analyses.

Due to the strong similarity of the XRD patterns of the apatite group members (Supplemental Data Figure SD5), the choice of the reference patterns for the phase identification should be carefully considered. For this purpose, the following ICDD (International Centre for Diffraction Data) patterns of HAp (PDF code 00-009-0432), FAp (PDF code 00-015-0876), ClAp (PDF code 00-033-0271) and carbonate-apatite (CarbAp, PDF code 00-019-0272) have been selected because they were collected from synthetic samples and match the Star quality mark (i.e. well characterized chemically and crystallographically pattern, no unindexed

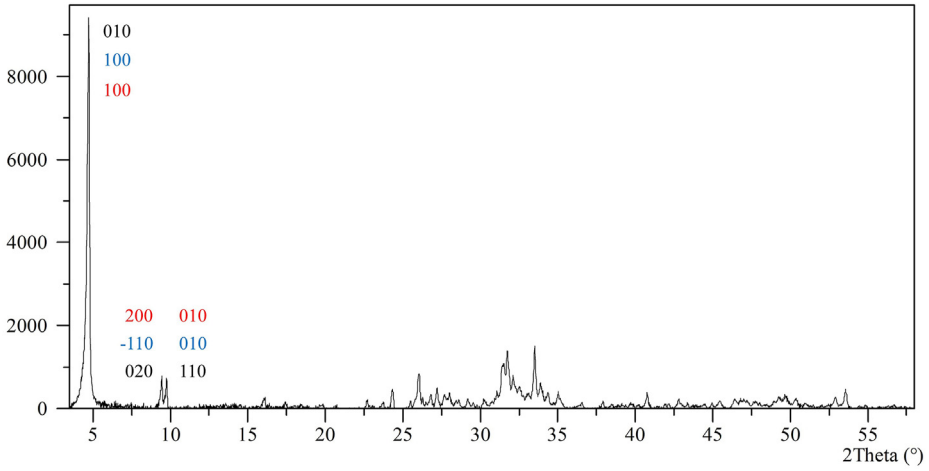

Figure 1. XRD pattern of the OCP used in the experiments. The indexed reflections written in black font are from Brown (1962), those in blue are from Frazier et al. (1991), and those in red are from the present study.

Table 1. Crystallographic parameters of OCP for a Triclinic system.

a	b	c	α	β	γ	V	Reference
Å			(°)			10^6 pm^3	
9.259	18.994	6.855	92.33	90.13	79.93	1220.57	Brown (1962)
19.87	9.63	6.875	89.28	92.22	108.95	1243.29	Frazier et al. (1991)
19.70	9.50	6.85	90.03	92.48	108.3	n.r.	Arellano-Jiménez et al. (2009)
20.37	9.78	4.76	90.70	92.90	113.2	868.4	present study

n.r. = not reported.

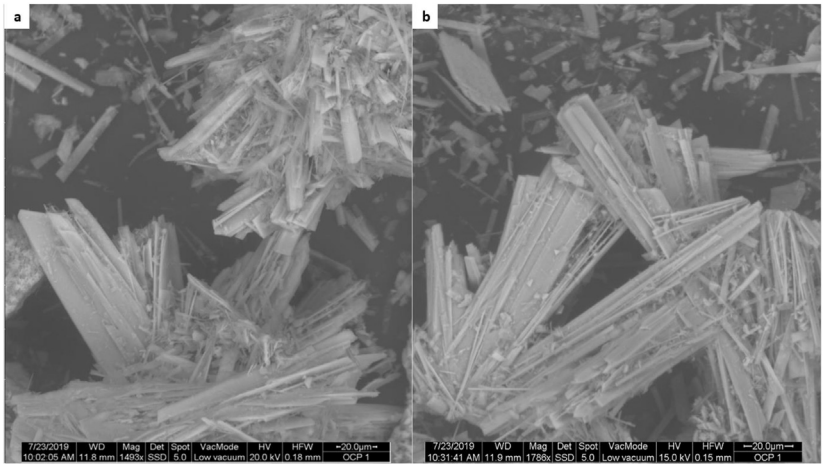

Figure 2. Two ESEM images of the synthesized OCP used for the anionic competition experiments: a) radial crystal aggregates; b) crystals with prismatic bladed habitus.

Table 2. Initial and final pH and dissolved anionic concentrations in the competition experiments of OCP transformation into apatite.

Experiment	pH		OH^- (mmol/L)		F^- (mmol/L)		Cl^- (mmol/L)		Alk (mmol/L)	
	initial	final	initial	final	initial	final	initial	final	initial	final
No_Comp	7.00	7.08	$1\ 10^{-4}$	$1.20\ 10^{-4}$	7.37	1.43	0	0	0	0
Cl_Comp	7.00	6.91	$1\ 10^{-4}$	$8.13\ 10^{-5}$	7.37	1.77	7.37	7.02	0	0
OH_Comp	11.87	7.26	7.37	$1.82\ 10^{-4}$	7.37	2.34	0	0	0	0
Alk_Comp	8.80	7.79	$6.31\ 10^{-3}$	$6.17\ 10^{-4}$	7.37	1.57	0	0	7.37	7.22
Tot_Comp	11.87	7.84	7.37	$6.92\ 10^{-4}$	7.37	2.09	7.37	7.07	7.37	7.18

Alk = $HCO_3^- + CO_3^{2-}$.

lines, $\Delta 2\theta \leq 0.03°$). The phase identification was carried out using the Rietveld algorithm that adopts the following agreement parameters (David, 2004):

$$R_{exp} = \sqrt{(N-P) \Big/ \sum_{i=1}^{N} w_i \left(y_j - b_i\right)^2} \quad (2)$$

Table 3. Measured amounts of F^- removed, P^{5+} and Ca^{2+} dissolved, and F^- empirical removal capacity (q_e) in the anionic competition experiments, compared with the theoretical values of the OCP transformation into FAp (React. 1 in the text). The No_Comp experiment is taken as a reference (100 % F^- removed) for the other experiments, and the relative percentages (%) are reported.

Experiment	F^- removed		q_e	P^{5+} dissolved	Ca^{2+} dissolved
	mmol	%	*mol/mol*	*mmol*	*mmol*
No_Comp	0.30	100	1.33	0.30	0.03
Cl_Comp	0.28	93	1.24	0.31	0.04
OH_Comp	0.25	83	1.10	0.32	0.03
Alk_Comp	0.29	97	1.29	0.31	0.03
Tot_Comp	0.24	80	1.06	0.33	0.04
OCP → FAp reaction	0.357		1.6	0.267	0

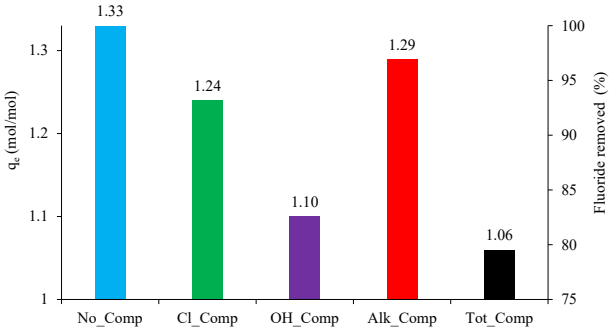

Figure 3. Plot of the fluoride empirical removal capacity (q_e) and percentage of fluoride removed for each anionic competition experiment. The No_Comp experiment is taken as a reference (100 % fluoride removed) for the other experiments.

$$R_{wp} = \sqrt{\sum_{i=1}^{N}[w_i(y_i - M_i)^2] \Big/ \sum_{i=1}^{N} w_i(y_j - b_i)^2} \quad (3)$$

$$GoF = \left(\frac{R_{wp}}{R_{exp}}\right)^2 \quad (4)$$

where R_{exp} (Eq. 2) is the statistical expected value of the dataset and represents the maximum possible agreement value; R_{wp} (Eq. 3) is the weighted profile, which is the statistical square root difference of the quantity minimized, scaled by the weighted intensities; *GoF* (Goodness of Fit) (Eq. 4) is the numerical evaluation of the fit, and its minimum value should be 1; N is the number of points and P the number of varied parameters; w, y, M and b are respectively the weight, the intensity, the calculated intensity and the background intensity at step i (David, 2004).

The results of the Rietveld method applied for the phase identification are listed in Table 4 and indicate that FAp is the phase that better fits all the experimental patterns, followed by HAp, while CarbAp and ClAp show a worse agreement. The good fit for HAp can be related to the co-occupancy of OH^- and F^- in the X site of apatite in all the experiments, while the co-occupancy seems to be more difficult for Cl^-. About the CarbAp poor fit, the entry of the carbonate anion in place of the phosphate one, and the consequent formation of carbonate-apatite, could also be inhibited by an excess of dissolved phosphate. It is worth saying that the aim of the Rietveld calculations here presented is just to compare the different fits for the apatite group end-members and not a refinement of their structures, since in the latter case better R_{wp} (<10) and *GoF* (~2) values would be required.

The cell parameters, calculated using the McMaille algorithm (Le Bail, 2004), show that all the solid phases can be solved in the Hexagonal system (space group P 6_3/m); the values show small differences among them (Table 5) and are close to the cell parameters of the apatite group end-members (e.g. fluorapatite from MinDat (https://www.mindat.org/min-1572.html) has a = 9.3973 Å, c = 6.8782 Å, V = 526.03 · 10^6 pm^3).

The ESEM images of the solid phases collected at the end of all the anionic competition experiments show aggregates of acicular crystals (Figure 5a,b,c), indicating a clear morphological change with respect to the OCP crystals shown in Figure 2. Moreover, the EDS analyses (Figure 5d and Figure SD6 in the Supplemental Data) indicate that, in addition to O, the only elements identified are Ca,

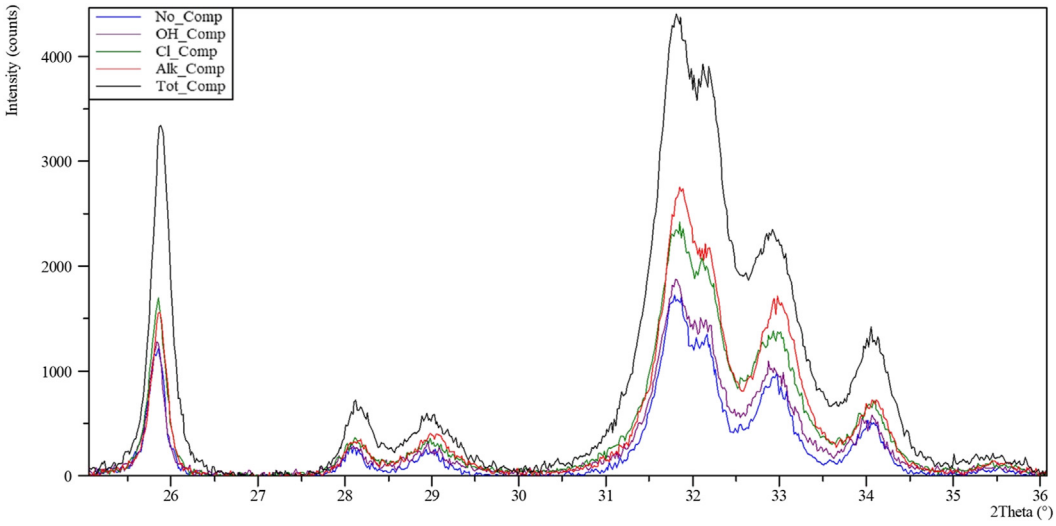

Figure 4. Selected portion of X-ray diffraction patterns of the solid phases collected at the end of the anionic competition experiments.

Table 4. Results of the Rietveld method applied for the identification of the solid phases collected at the end of the anionic competition experiments. See the text for the meaning of the tabulated parameters and labels.

Phase	No_Comp			OH_Comp			Cl_Comp			Alk_Comp			Tot_Comp		
	R_{wp}	R_{exp}	*GoF*	R_{wp}	R_{exp}	*GoF*	R_{wp}	R_{exp}	*GoF*	R_{wp}	R_{exp}	*GoF*	R_{wp}	R_{exp}	*GoF*
FAp	10.394	5.148	*4.076*	9.232	4.273	*4.668*	10.295	5.181	*6.747*	9.156	4.31	*4.51*	9.542	3.070	*9.355*
HAp	10.788	5.148	*4.391*	9.477	4.273	*4.918*	13.562	5.181	*6.853*	9.520	4.31	*4.87*	9.763	3.070	*9.986*
ClAp	-	-	-	-	-	-	15.258	5.181	*9.894*	-	-	-	9.815	3.070	*10.219*
CarbAp	-	-	-	-	-	-	-	-	-	11.62	4.23	*7.55*	14.094	3.089	*20.814*

Table 5. Cell parameters calculated for the solid phases collected at the end of the anionic competition experiments. At least 22 XRD reflections with 2 % minimum relative intensity were used for calculations. The cell parameters refer to the Hexagonal system (space group P 6_3/m).

Experiment	a	c	α	β	γ	V	Indexed reflections
	Å		(°)			10^6 pm^3	(unindexed)
No_Comp	9.401	6.889	90	90	120	527.33	24 (0)
Cl_Comp	9.415	6.895	90	90	120	529.37	22 (0)
OH_Comp	9.405	6.889	90	90	120	527.81	32 (0)
Alk_Comp	9.402	6.887	90	90	120	527.30	29 (0)
Tot_Comp	9.416	6.884	90	90	120	528.36	28 (0)

P and F, and their intensity ratios are constant along the points analysed, confirming that the phase formed through OCP transformation in the presence of various dissolved anions (F^-, Cl^-, OH^-, (HCO_3^- + CO_3^{2-})) is mainly a fluorapatite (FAp).

3.4. Chemical analysis and mineral chemistry of solid phases

The wet chemical analysis of the solid phases collected at the end of the anionic competition experiments was performed after the acidic dissolution of 150 mg of each sample in 1 L of deionized water. The results (Table 6) have been interpreted on the basis of the following general crystallochemical formula for the apatite group minerals: $M_5(TO_4)_3X$, where M = Ca^{2+}, T = P^{5+}, X = F^-, Cl^-, OH^-.

The concentrations of Ca and P are quite similar in all solid phases (Ca = 58.81–59.13 mg/L; P = 26.67–27.57 mg/L). The low concentrations of Na (0.72–1.28 mg/L) measured in all samples are due to the possible Ca ⇆ Na substitution in the M site. All solid phases contain F^-, the highest concentration is in the No_Comp experiment sample (5.13 mg/L), the lowest one in the OH_Comp experiment sample (4.28 mg/L). Very low Cl^- concentrations were detected only in the solids of the Cl_Comp (0.92 mg/L) and Tot_Comp (0.53 mg/L) experiments.

The chemical composition expressed in wt. % of oxides and elements (Table 6) clearly converges towards the stoichiometric mineral chemistry of FAp. The calculation of the atoms per formula unit (a.p.f.u.), performed using the Apatite Calculation Sheet by ©Gabbrosoft 2011 and following the recommendations of Pasero et al. (2010), shows that there is a deficiency in the T site and an excess of positive charge (Table 6), even perfectly filling the X site up to the value of 1 with the addition of OH^-. In order to balance the excess of positive charge, it was assumed the contribution of the carbonate anion both from atmospheric CO_2 dissolved in water and from $NaHCO_3$ salt used in the Alk_Comp and Tot_Comp experiments. The possible PO_4^{3-} ⇆ CO_3^{2-} substitution (Awonusi et al., 2007) was considered at an extent sufficient to obtain a perfect charge balance, and the resulting calculation is close to the theoretical value of 3 for the T site. The M site, occupied by Ca^{2+} and Na^+, is close to the expected value of 5.

4. Experimental summary and discussion

The results of the No_Comp experiment show that OCP reacts in the presence of F^- to form FAp. The OCP → FAp reaction also occurs in the presence of single competing anions (i.e. OH^-, Cl^- or (HCO_3^- + CO_3^{2-})) at

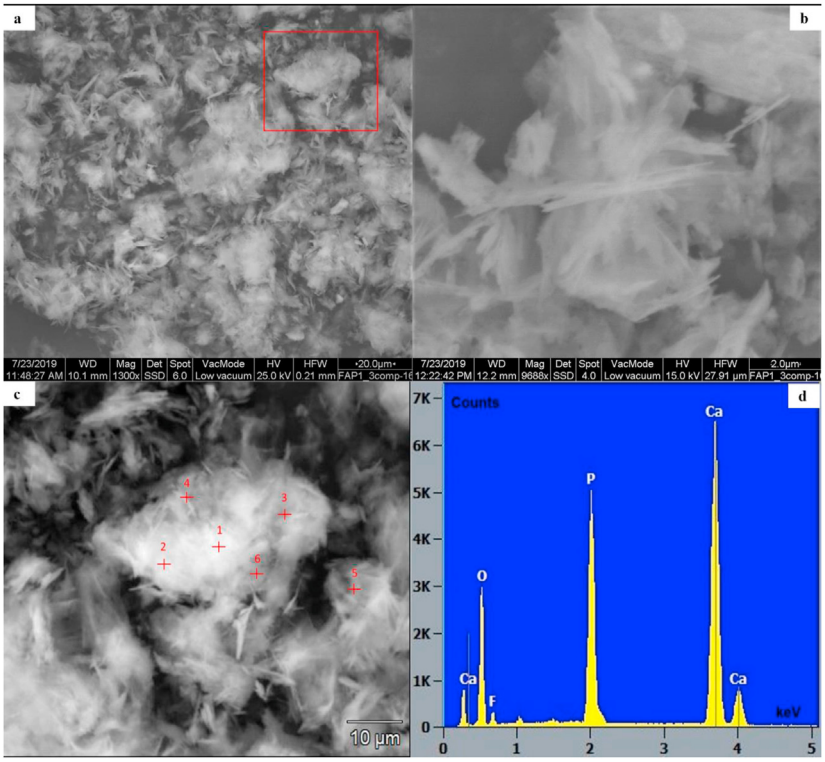

Figure 5. ESEM images and EDS spectrum of the solid phase collected at the end of the anionic competition experiment Tot_Comp: a) aggregate of fluorapatite (FAp) acicular crystals, the red square is one of the areas analysed by EDS; b) magnification of FAp aggregates; c) magnification of FAp aggregates within the red square in a) with the EDS analysis spots (see Figure SD6 in the Supplemental Data for the EDS spectra); d) example of EDS spectrum with elemental identification.

Table 6. Wet chemical analysis (concentrations in mg/L), chemical composition (concentrations in wt. %) and atom per formula unit (a.p.f.u.) calculation of the solid phases collected at the end of the anionic competition experiments. FAp_{th} indicates the theoretical values for fluorapatite. The general crystallochemical formula used for the apatite group minerals is $M_5(TO_4)_3X$.

	Wet chemical analysis (mg/L)					
	No_Comp	Cl_Comp	OH_Comp	Alk_Comp	Tot_Comp	
Ca	59.03	59.13	58.81	59.12	58.92	
Na	1.28	1.20	1.38	0.93	0.72	
P	27.07	26.95	27.57	26.67	26.95	
Cl	0.00	0.92	0.00	0.00	0.53	
F	5.13	4.73	4.28	5.00	4.56	
	Chemical composition (wt. %)					
	No_Comp	Cl_Comp	OH_Comp	Alk_Comp	Tot_Comp	FAp_{th}
CaO	55.06	55.16	54.86	55.15	54.96	55.60
Na_2O	1.15	1.08	1.24	0.84	0.65	
P_2O_5	41.35	41.17	42.12	40.74	41.16	42.22
Cl	0.00	0.61	0.00	0.00	0.35	
F	3.42	3.15	2.85	3.33	2.64	3.77
Sub-Total	100.98	101.17	101.07	100.06	99.76	101.59
$-O=F_2,Cl_2$	1.44	1.46	1.20	1.40	1.19	1.59
Total	99.54	99.71	99.87	98.66	98.57	100
	atom per formula unit (a.p.f.u.)					
	No_Comp	Cl_Comp	OH_Comp	Alk_Comp	Tot_Comp	FAp_{th}
Ca	4.819	4.835	4.782	4.879	4.871	5
Na	0.182	0.171	0.196	0.134	0.104	
P	2.859	2.852	2.901	2.848	2.883	3
Cl	0.000	0.085	0.000	0.000	0.050	
F	0.883	0.815	0.733	0.843	0.691	1
OH	0.117	0.100	0.267	0.157	0.259	
Charge Balance	+0.243	+0.285	+0.057	+0.348	+0.197	
Charge Balance + (CO_3)	0	0	0	0	0	
M site (Ca + Na)	5.001	5.006	4.978	5.013	4.975	5
T site (P)	2.859	2.852	2.901	2.848	2.883	3
T site + (CO_3)	2.980	2.994	2.930	3.022	2.982	
X site (F + Cl + OH)	1.000	1.000	1.000	1.000	1.000	1

the same dissolved concentration of F^- (respectively, OH_Comp, Cl_Comp and Alk_Comp experiments), and even when the competing anions are all simultaneously present in solution at the same concentration (Tot_Comp experiment) (Tables 2, 3, and 6). The possibility of precipitation of F-bearing phases other than FAp (e.g. fluorite CaF_2, whose XRD pattern overlaps that of FAp) was excluded by observation of the crystal morphology from ESEM images and the semi-quantitative chemical analyses from EDS spectra (Figures 2 and 5). The application of the Rietveld algorithm to the XRD patterns from the solid phases collected at the end of the anionic competition experiments confirms FAp as the main phase, followed by HAp, in every experiment (Table 4). The calculation of cell parameters for all solid phases provides very similar values (Table 5) that can be solved in the Hexagonal system and are close to the cell parameters of the apatite group end-members.

Considering the theoretical OCP → FAp transformation (React. 1), our results show two main, though not fundamental, differences. The first one concerns the amount of F^- removed from solution: in the No_Comp experiment, the amount of F^- removed is 0.30 mmol (Table 3), while the stoichiometry of the reaction indicates 0.357 mmol; the second difference concerns the presence of some Ca in solution (0.03–0.04 mmol) and the amount of dissolved P, that ranges from 0.30 to 0.33 mmol and is about 17.6 % higher than the expected value of 0.267 mmol (Table 3). The excess of P and the presence of Ca in solution, that should be related to the solubility product (K_{sp}) of FAp at the experimental conditions, indicate that at least 0.01 mmol of FAp is missing from the theoretical expected value of 0.357 mmol and, consequently, 0.01 mmol of F^- was not removed. The other effect that affects the uptake of F^- is the occupancy of the X site of apatite by OH^-: the a.p.f.u. calculations indicate that OH^- occupies up to 11.7 % of the X site in the No_Comp experiment solid, while in the OH_Comp experiment solid the percentage of occupancy reaches 26.7 % (Table 6).

The Cl^- competition has a very limited effect on the uptake of F^- (93 % of F^- removed in the Cl_Comp experiment, Table 3), but also the OH^- competition affects the Cl^- entry into the X site. In fact, the chemical analysis and the a.p.f.u. calculation of the Cl_Comp experiment solid show that the X site occupancy is 81.5 % F^-, 8.5 % Cl^- and 10 % OH^- (Table 6). The poor affinity of Cl^- can be explained by two reasons: (i) FAp is thermodynamically more stable than ClAp (Drouet, 2015) and (ii) F^- can occupy the same crystallographic position of Cl^- but not vice versa (Hughes et al., 2014).

The effect of carbonate species on F^- uptake in the Alk_Comp experiment is very limited (97 % of F^- removed, Table 3). Actually, the possible role of CO_3^{2-} concerns more the T site, due to the $PO_4^{3-} \rightleftharpoons CO_3^{2-}$ substitution, rather than the X site for a hypothetical (F^-, Cl^-, OH^-) $\rightleftharpoons CO_3^{2-}$ substitution, as discussed by Awonusi et al. (2007).

In the Tot_Comp experiment, where all the competing anions are tested simultaneously, the F^- removed decreases to 80 % (Table 3), and the a.p.f.u. calculation of the corresponding FAp shows that OH^- is always the main competitor of F^- (X site occupancy 26 %, Table 6).

Another effect observed in the OCP → FAp reaction is that the final pH tends to circum-neutral values, regardless of the initial OH^-

concentration (Table 2). The OH^- neutralization can be explained by a different mechanism other than the ingress of OH^- in the FAp structure: the OCP → FAp reaction releases H^+ and monohydrogenphosphate (HPO_4^{2-}) into solution. The dissociation constants (pKa2 and pKa3) of hydrogen phosphate species according to the following React. (2) and React. (3):

$$H_2PO_4^- \rightleftharpoons HPO_4^{2-} + H^+ \quad pKa2 = 7.20 \qquad \text{(React 2)}$$

$$HPO_4^{2-} \rightleftharpoons PO_4^{3-} + H^+ \quad pKa3 = 12.37 \qquad \text{(React 3)}$$

indicate that $H_2PO_4^-$ and HPO_4^{2-} are the main species present in solution at circum-neutral pH values such as those measured at the end of the anionic competition experiments (Table 2). Moreover, the stability of $H_2PO_4^-$ is strongly affected by the formation of the ion-pair $NaHPO_4^-$ (Na^+ is from NaF salt used to provide F^- in solution) that can bind up to 19 % of dissolved HPO_4^{2-}, as in the case of apatite supersaturation condition. Consequently, the subtraction of HPO_4^{2-} by complexation with Na^+ moves React. (2) to the right, generating more H^+ in solution (Patel et al., 1974).

As mentioned in the Introduction, the use of OCP as the precursor of FAp for removing F^- from groundwater has been documented. The experimental evidence suggests that OCP can be used as a precursor of FAp also in the presence of strong anionic competitors other than F^-. Conversely, the release of P from the OCP → FAp reaction should be taken into account to avoid an environmental adverse effect. For instance, the addition of Ca^{2+}, using soluble Ca-salts such as CaO or $Ca(OH)_2$, could bind dissolved PO_4^{3-} and F^- (and/or OH^-), so triggering the precipitation of FAp thanks to its low K_{sp} (Wei et al., 2013).

Finally, on the basis of a.p.f.u. calculations (Table 6), the empirical formula of each experimental phase can be written as follows:

$$No\_Comp = Ca_{4.819}Na_{0.182}(PO_4)_{2.859}(CO_3)_{0.122}(F_{0.883},OH_{0.117})$$

$$Cl\_Comp = Ca_{4.835}Na_{0.171}(PO_4)_{2.852}(CO_3)_{0.142}(F_{0.815},OH_{0.100},Cl_{0.085})$$

$$OH\_Comp = Ca_{4.782}Na_{0.196}(PO_4)_{2.901}(CO_3)_{0.028}(F_{0.733},OH_{0.267})$$

$$Alk\_Comp = Ca_{4.879}Na_{0.134}(PO_4)_{2.848}(CO_3)_{0.174}(F_{0.843},OH_{0.157})$$

$$Tot\_Comp = Ca_{4.871}Na_{0.104}(PO_4)_{2.883}(CO_3)_{0.098}(F_{0.691},OH_{0.259},Cl_{0.050})$$

5. Conclusions

The reactivity of 0.223 mmol of octacalcium phosphate (OCP, $Ca_8(HPO_4)_2(PO_4)_4 \cdot 5H_2O$) in 50 mL aqueous solution has been tested in the presence of 0.368 mmol of F^-, Cl^-, OH^- and ($HCO_3^- + CO_3^{2-}$). The results of the anionic competition experiments indicate that dissolved F^- is the anion mostly removed from solution in every experiment, and the removal efficiency decreases by 20 % when all the anions are present in solution simultaneously.

Crystallographic and crystal chemistry analyses indicate that in the transformation reaction of OCP into apatite, the main apatitic phase formed is always fluorapatite (FAp, $Ca_5(PO_4)_3F$). The crystallochemical analysis of the resulting FAp indicates that OH^- is the most important competitor of F^-, especially when the OCP → FAp reaction occurs at uncommon high pH values (pH ~ 12).

From experimental evidence, it can be said that OCP is a crystalline precursor of apatite and can be used to efficiently remove dissolved F^- from fluoride-rich water by forming FAp even in the presence of high concentrations of possible anionic competitors. These peculiar features of OCP could also contribute to the environmental research on the use of apatite for the uptake of toxic metals through the ion-exchange property of the M site (e.g. $Ca^{2+} \rightleftharpoons Pb^{2+}$, $Ca^{2+} \rightleftharpoons Cd^{2+}$, etc.).

Declarations

Author contribution statement

Alfredo Idini: Conceived and designed the experiments; Performed the experiments; Analyzed and interpreted the data; Contributed reagents, materials, analysis tools or data; Wrote the paper.

Franco Frau: Conceived and designed the experiments; Analyzed and interpreted the data; Contributed reagents, materials, analysis tools or data; Wrote the paper.

Funding statement

This work was supported by the FLOWERED project (Coordinator Giorgio Ghiglieri, University of Cagliari, Italy), a Horizon2020 program funded by the European Commission (Grant Agreement N. 690378) (www.floweredproject.org). This work was also supported by MIUR (Ministry of University and Research of the Italian Government) through a PhD grant to Alfredo Idini (Grant Code DOT1304527-1) in the frame of PON R&I 2014-2020 "Innovative doctorates with industrial characterization.

Data availability statement

Data included in article/supplementary material/referenced in article.

Declaration of interests statement

The authors declare no conflict of interest.

Additional information

Supplementary content related to this article has been published online at https://doi.org/10.1016/j.heliyon.2021.e06882.

Acknowledgements

We wish to thank Francesca Podda and Dario Fancello from the University of Cagliari (Italy) for their helpful support with the ESEM and ICP-OES analyses.

References

Arellano-Jiménez, M.J., García-García, R., Reyes-Gasga, J., 2009. Synthesis and hydrolysis of octacalcium phosphate and its characterization by electron microscopy and X-ray diffraction. J. Phys. Chem. Solid. 70 (2), 390–395.

Awonusi, A., Morris, M.D., Tecklenburg, M.M.J., 2007. Carbonate assignment and calibration in the Raman spectrum of apatite. Calcif. Tissue Int. 81 (1), 46–52.

Ayoob, S., Gupta, A.K., 2006. Fluoride in drinking water: a review on the status and stress effects. Crit. Rev. Environ. Sci. Technol. 36 (6), 433–487.

Boultif, A., Louër, D., 2004. Powder pattern indexing with the dichotomy method. J. Appl. Crystallogr. 37 (5), 724–731.

Brown, W.E., 1962. Octacalcium phosphate and hydroxyapatite: crystal structure of octacalcium phosphate. Nature 196, 1048–1050.

Carino, A., Ludwig, C., Cervellino, A., Müller, E., Testino, A., 2018. Formation and transformation of calcium phosphate phases under biologically relevant conditions: experiments and modelling. Acta Biomater. 74, 478–488.

David, W.I.F., 2004. Powder diffraction: least-squares and beyond. J. Res. Natl. Inst. Stand. Technol. 109 (1), 107–123.

Dorozhkin, S.V., 2016. Multiphasic calcium orthophosphate ($CaPO_4$) bioceramics and their biomedical applications. Ceram. Int. 42 (6), 6529–6554.

Drouet, C., 2015. A comprehensive guide to experimental and predicted thermodynamic properties of phosphate apatite minerals in view of applicative purposes. J. Chem. Thermodyn. 81, 143–159.

Everett, E.T., 2011. Fluoride's effects on the formation of teeth and bones, and the influence of genetics. J. Dent. Res. 90 (5), 552–560.

Fawell, J., Bailey, K., Chilton, J., Dahi, E., Fewtrell, L., Magara, Y., 2006. Fluoride in Drinking-Water. IWA Publishing, London (UK), pp. 1–144 on behalf of World Health Organisation (WHO). http://www.who.int/water_sanitation_health/publications/fluoride_drinking_water_full.pdf. (Accessed 8 April 2021).

Frazier, A.W., Dillard, E.F., Thrasher, R.D., Waerstad, K.R., Hunter, S.R., Kohler, J.J., Scheib, R.M., 1991. Crystallographic Properties of Fertilizer Compounds. Technical Report, TVA-Bulletin Y-217, TVA/NFERC-91/4, USA, pp. 1–983.

Hughes, J.M., Nekvasil, H., Ustunisik, G., Lindsley, D.H., Coraor, A.E., Vaughn, J., Phillips, B.L., McCubbin, F.M., Woerner, W.R., 2014. Solid solution in the fluorapatite-chlorapatite binary system: high-precision crystal structure refinements of synthetic F-Cl apatite. Am. Mineral. 99 (2–3), 369–376.

Hughes, J.M., Rakovan, J.F., 2015. Structurally robust, chemically diverse: apatite and apatite supergroup minerals. Elements 11 (3), 165–170.

Idini, A., Dore, E., Fancello, D., Frau, F., 2019. Defluoridation of water through the transformation of octacalcium phosphate into fluorapatite. Heliyon 5 (8), e02288, 1-9.

Idini, A., Frau, F., Gutierrez, L., Dore, E., Nocella, G., Ghiglieri, G., 2020. Application of octacalcium phosphate with an innovative household-scale defluoridator prototype and behavioral determinants of its adoption in rural communities of the East African Rift Valley. Integrat. Environ. Assess. Manag. 16 (6), 856–870.

Jarvis, I., Burnett, W.C., Nathan, Y., Almbaydin, F.S.M., Attia, A.K.M., Castro, L.N., Flicoteaux, R., Ezzeldim Hilmy, M., Husain, V., Qutawnah, A.A., Serjani, A., Zanin, Y.N., 1994. Phosphorite geochemistry: state-of-the-art and environmental concerns. Eclogae Geol. Helv. 87 (3), 643–700.

Le Bail, A., 2004. Monte Carlo indexing with McMaille. Powder Diffr. 19 (3), 249–254.

Ozsvath, D.L., 2009. Fluoride and environmental health: a review. Rev. Environ. Sci. Biotechnol. 8, 59–79.

Pasero, M., Kampf, A.R., Ferraris, C., Pekov, I.V., Rakovan, J., White, T.J., 2010. Nomenclature of the apatite supergroup minerals. Eur. J. Mineral 22 (2), 163–179.

Patel, P.R., Gregory, T.M., Brown, W.E., 1974. Solubility of $CaHPO_4 \cdot 2H_2O$ in the quaternary system $Ca(OH)_2$ - H_3PO_4 - NaCl - H_2O at 25 °C. J. Res. NBS, Sect. A: Phys. Chem. 78A (6), 675–681.

Rakovan, J.F., Pasteris, J.D., 2015. A technological gem: materials, medical, and environmental mineralogy of apatite. Elements 11 (3), 195–200.

Sakae, T., Nakada, H., LeGeros, J.P., 2015. Historical review of biological apatite crystallography. J. Hard Tissue Biol. 24 (2), 111–122.

Smith, G.S., Snyder, R.L., 1979. F_N : a criterion for rating powder diffraction patterns and evaluating the reliability of powder-pattern indexing. J. Appl. Crystallogr. 12 (1), 60–65.

Suzuki, O., 2013. Octacalcium phosphate (OCP)-based bone substitute materials. Jpn. Dent. Sci. Rev. 49 (2), 58–71.

Wei, C., Zhu, Y., Yang, F., Li, J., Zhu, Z., Zhu, H., 2013. Dissolution and solubility of hydroxylapatite and fluorapatite at 25°C at different pH. Res. J. Chem. Environ. 17 (11), 57–61.

Wopenka, B., Pasteris, J.D., 2005. A mineralogical perspective on the apatite in bone. Mater. Sci. Eng. C 25, 131–143.

Xin, R., Leng, Y., Wang, N., 2006. In situ TEM examinations of octacalcium phosphate to hydroxyapatite transformation. J. Cryst. Growth 289 (1), 339–344.